

## Electron-impact dissociative double ionization of $N_2$ and CO: Dependence of transition probability on impact energy

A. Pandey,<sup>1,\*</sup> P. Kumar,<sup>1</sup> S. B. Banerjee,<sup>1</sup> K. P. Subramanian,<sup>1</sup> and B. Bapat<sup>2</sup>

<sup>1</sup>*Physical Research Laboratory, Ahmedabad 380009, India*

<sup>2</sup>*Indian Institute of Science Education and Research Pune, India*

(Received 2 February 2016; published 28 April 2016)

We present an experimental and computational analysis of dissociative double ionization of  $N_2$  and CO molecules under electron impact. Experiments are performed at three energies, viz. 1, 3, and 5 keV, in order to observe the effect of impact energy on the dissociative ionization kinematics. We compare the kinetic energy release (KER) distributions of the charge symmetric dissociation channels of  $N_2^{2+}$  and  $CO^{2+}$  at these impact energies. An approximately linear trend between the transition energy and the expected KER values is inferred on the basis of the calculated potential energy curves of the dications. Experimentally, the normalized differential KER cross sections for these channels show an increasing trend in the low KER range and a decreasing trend in the high KER range as the electron-impact energy is increased. This observation indicates that the transition probability for excitation to different molecular ion states is not only a function of energy difference between the ground and excited states, but also a complicated function of the impact energy. In addition, nature of the observed trend in the differential KER cross sections differs significantly from their differential transition probability, which are calculated using inelastic collision model for fast-electron-impact case.

DOI: [10.1103/PhysRevA.93.042712](https://doi.org/10.1103/PhysRevA.93.042712)

### I. INTRODUCTION

In a molecular collision process, large differences in time scales of the electronic and the nuclear dynamics allow one to treat ionization and following evolution of the molecular ion separately. This specific property of the molecular system leads one to consider many assumptions and approximations, like vertical transition, adiabatic approximation, etc., which are used to construct the molecular picture [1–3]. In the ionizing collisions, these approximations can be divided in two categories: one which addresses the excitation process and the other energy dissipation and dynamics of the system after electronic excitation. However, often in these processes, the composite kinematics is observed and, for this reason, the underlying set of approximations and assumptions can be probed only jointly. As a result, some characteristics of electronic excitation and nuclear dynamics which are not having strong influence in the final kinematics cannot be discerned.

In the study of dissociative ionization processes, electronic excitation which leads to ionization of the molecular system and the following nuclear dynamics are normally treated as two separate processes; the average time scale difference between ionization and the nuclear dynamics of the molecular ions is of three orders of magnitude [4,5]. With this view, a dissociative ionization process is described as a two step process: a molecular system first gets ionized and then dissociates. Since the dissociation always preceded by ionization of the parent molecular system, the kinematical study of the fragmentation of molecular ion inevitably inherits properties of ionization. Probability of the transition in a given potential energy state, normally termed as transition probability, of the molecular ion is the parameter which manifests the properties of ionization. Apart from the dependence on symmetry of excited states,

transition probability is assumed to be strongly dependent on the transition energy: the energy required to reach the excited potential energy curve (PEC) of ionized molecular ion from the ground state of neutral molecule in vertical transition and weakly dependent on the impact energy. For the high impact nonresonant excitation processes, transition probability becomes a uniparameter function of the transition energy: an inverse quadratic function [6]. In this paper, we try to examine the nature of the transition probability as a function of impact energy of the projectile.

Total ionization cross section of many atomic and molecular systems at different electron-impact energies have been studied quite extensively in the past, theoretically as well as experimentally [7–11]. From these studies, it can be observed that below 80 eV, the total ionization cross section of molecular systems are normally a rising function. Above 100 eV, the cross section becomes a falling function of the impact energy. In energy range above 1000 eV, the total cross section for all molecular systems are a weak falling function which is almost similar for all molecules irrespective to their molecular structures.

Kinematics observed in charge symmetric dissociation (CSD) of dications of  $N_2$  and CO molecules upon electron impact of few keV energy span PECs in the range 40–60 eV above the ground state [12–14]. Experimental and theoretical investigation of dissociation dynamics of these channels have been thoroughly studied recently as well as in the past for many ionizing agents [12–26]. It has been found that dissociation dynamics of these two systems are significantly different and that has been attributed to the intrinsic symmetry of their molecular states. Extensive knowledge of the dynamics of dissociative ionization of these dications provides a solid ground to examine questions about their excitation processes. In addition, participation of the excited states of  $N_2^{2+}$  and  $CO^{2+}$  which span more than 20 eV energy range, from 40–60 eV, creates a good opportunity to expect some variation, if any, because of dependence on the impact energy.

\*amrendra@prl.res.in

In this article, we compare KER spectra of CSD channels of these dications for three electron-impact energies and have observed a common trend for both molecular ions. We reason that the resultant trend in the intensity pattern of the KER spectra must be arising from the properties of ionization, i.e., differences in their transition probabilities rather than the variation in dynamics of the dissociation at different impact energies. It is suggested that the transition probability should be a decreasing function of the electron-impact energy.

## II. EXPERIMENT

Experiments are performed employing Recoil Ion Momentum Spectrometer (RIMS) to record ionizing collision products of  $N_2$  and CO molecules at three electron-impact energies: 1, 3, and 5 keV. In the setup, molecules forming an effusive beam collide with electron beam in cross-beam geometry resulting in an ionization region of volume less than  $3 \text{ mm}^3$ . A constant electric field over 11 cm from the ionization region, called the extraction region, is applied to extract the positive ions created in the collision. A field-free region, drift region, of 22 cm is used after the extraction region to achieve the first-order space focusing Wiley-McLaren condition [27]. Electrons created in ionization are directed in the opposite direction and detected by a microchannel plate (MCP). They are used as a start for recording time-of-flight of ions that reach the ion detector. In the ion side, a MCP along with delay-line detector is used to detect the ions. For each ion detected, time-of-flight (TOF), and their positions, two perpendicular coordinates with respect to spectrometer axis,  $(X, Y)$ , on the detector are recorded in a list mode format. These parameters are used to calculate the momentum components  $(P_x, P_y, P_z)$  of ions. Kinetic energy of ions are estimated using their measured momentum components. RIMS operates in multihit coincidence, four-hit in our case, and thus is capable of detecting ion pairs created in the collision process and it enables distinguishing dissociation channels of the detected ions in a single collision condition. KER of CSD of a  $N_2$  (or CO) dication is the sum of the kinetic energies of the fragmented ions, detected in coincidence [28,29].

Experiments are performed at 90 V/cm to minimize the transmission loss that causes alteration in the relative cross section of dissociation products in high KER range. Effect of transmission loss and its nature as a function of KER can be found in [30]. At 90 V/cm extraction field for RIMS setup, transmission loss for a single ion starts at 7.25 eV. In the case of fragmentation, in KER spectra, effect of transmission loss starts appearing when one of its fragments acquire more than 7.25 eV kinetic energy from dissociation. In two-body fragmentation, KER value at which loss will start can be calculated for any pair of fragments of known masses. In this case, geometry of the molecular system does not contribute which is the reason for an inability to derive the functional form of the transmission loss in many-body fragmentation. In the case of  $N_2^{2+}$  dissociating to  $N^+, N^+$ , KER value at which the transmission loss starts occurring is 14.50 eV, whereas in the case of CSD of  $CO^{2+}$ , it is 12.65 eV. In our case, only a little fraction of the total cross section falls above these KER values, and thus KER spectra in these cases are not corrected to transmission losses. Only 20% of the total cross section

falls above 14.5 eV KER in CSD of  $N_2^{2+}$  and 12.65 eV in the case of CSD of  $CO^{2+}$  for these electron-impact energies. The estimated increment in the total cross section after applying the transmission loss correction is less than 5% in each case. Apart from transmission loss, other correction factors like detector efficiency and ion transmission coefficients are also used to estimate the accurate cross section of dissociation channels [31–33]. Since we are interested in relative variation of the same dissociation channel at different impact energies, these correction factors are not necessary for our discussion and hence ignored.

To compare the kinematical differences of dissociation for three electron-impact energies, it is essential to establish that all experimental conditions were identical and any discernible experimental artifact cannot be a cause for the trend observed in KER spectra of  $N_2$  and CO dications. The first source of artifacts could be the change in the TOF of ions at different impact energies. In order to exclude this possibility, RIMS setup is optimized using argon gas at each electron-impact energy, i.e., minimizing the effect of finite position and initial velocity distributions of molecular ions in their TOF distributions. The observed calibration curves of Ar in optimized condition are identical; TOF(m/q) equations are similar indicating the fact that the ionization regions are identically situated in the RIMS in all cases. Any change in KER spectra because of the variation in the calibration curves would be negligible for the range in which the trends in the KER spectra have been observed. Experiments for  $N_2$  and CO are performed under the same conditions as for Ar.

The second source of artifact that may contribute to the KER spectra arise because of the finite distributions in two positions  $(X$  and  $Y)$  and TOF spectra of ions which are manifestations of the initial thermal and space distributions. In order to know these distributions, spectra of argon gas, which is monoatomic, are analyzed and they are found to be quite similar in all cases. At 3000 eV electron-impact energy, resolution of  $P_x$ ,  $P_y$ , and  $P_z$  momentum components of  $Ar^+$  ions are 30, 25, and 12 a.u., respectively. These momentum resolutions are calculated using full width at half maximum (FWHM) of the position and time distributions. Corresponding kinetic energy resolution of ions can be calculated using observed momentum resolutions and it turns out to be 300 meV. For two-body fragmentation, KER resolution can be estimated using kinetic energy resolution of ions as independent variables. It will be 430 meV. For all results, we have taken 500 meV as the resolution of the spectrometer for two-body fragmentation and only those features which sustain are considered as relevant. Calculation of KER resolution from the recorded TOF and  $(X, Y)$  distributions can be found in [29]. The procedure of the estimation of KER from the momentum components of the fragmented ions, recorded in coincidence, is identical to the study reported by Tarisien *et al.* [26]. In their case, however, better resolution in KER, less than 250 meV, is achieved because target molecules are introduced by a supersonic gas jet which has reduced interaction region and thermal width; for the supersonic beam, thermal width is much smaller than thermal width of the gas ensemble in an effusive beam, which we have used in our study.

Third and the last factor which can be a component in observed KER spectra is due to the strength of the

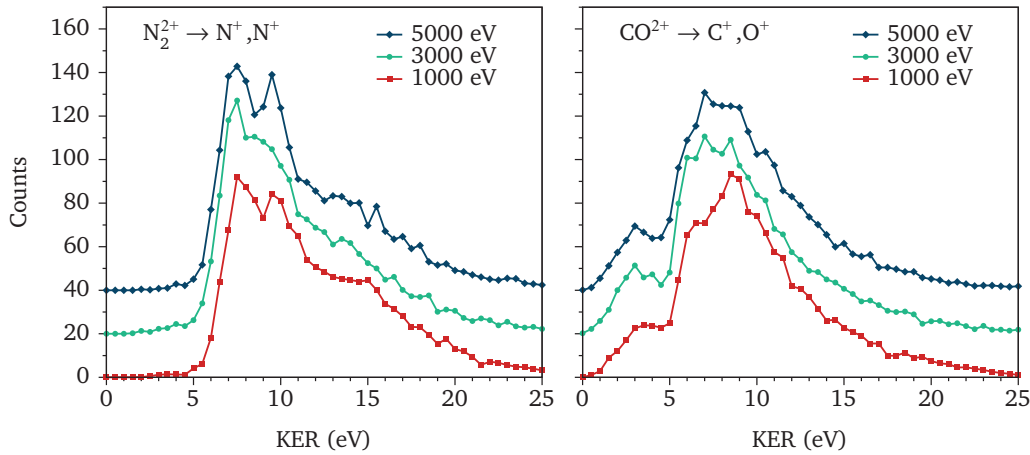


FIG. 1. Kinetic energy release spectra of CSD of  $N_2^+$  [left] and  $CO_2^+$  [right] are shown. For direct comparison, KER spectra for different electron-impact energies are normalized for their total cross section (area under curve). Relative variations can be compared for the features of normalized KER spectra. KER spectra are plotted with 500 meV bin size which represents the resolution for two-body dissociation channel. Features in KER spectra, in both molecular ions, appear at the same positions for different impact energies. Spectra observed at different impact energies are plotted with a shift of 20 for visual clarity.

observed statistics. In order to minimize the statistical errors, experiments are performed for a sufficiently long time. And in the entire observation period, precautions have been taken to maintain all the experimental conditions constant. Each run is performed for at least more than 18 h, resulting in a minimum of 7000 counts in CSD of  $N_2^+$  and about 12000 counts in CSD of  $CO_2^+$ . In all cases, counts at the maximum of a distribution is more than 500 (in the bin size of 500 meV). Statistical error for the range where counts are larger than 100 would be less than 0.1. The range of KER in which the observed counts are always bigger than 100 is about 12 eV, starting from 6 and going up to 18 eV for the  $N_2^+$  case. For  $CO_2^+$ , this is about 15 eV in the range 2–17 eV. Statistical error for these cases will not be more than 10% for these ranges. This suggests that any trend, if observed, having more differences than 10% would be resulting from the differences in the kinematics and cannot be attributed as experimental artifacts.

### III. RESULTS

KER spectra of CSD of  $N_2^+$  and  $CO_2^+$  for three electron-impact energies are shown in Fig. 1. KER spectra are plotted with 500 meV bin size which represents the resolution for two-body fragmentation. Spectra at each electron-impact energy is normalized to their total area under curve that is the absolute cross section of the CSD. Normalization is carried out to compare the relative intensities of the features in KER spectra. It can be easily observed that the main features appear at identical KER values in spectra for different electron-impact energies. In the case of CSD of  $N_2^+$ , the main features appear at 6.9 and 15 eV energies. Similarly, in the case of CSD of  $CO_2^+$ , the main features in KER spectra appear with common energies at 3, 6, and 9 eV. The appearance of features in KER spectra is associated with the dynamics on the excited PECs of molecular ions. Nature of the dynamical evolution for these two dissociation channels has been extensively worked out in the previous study [12]. From the available knowledge of the PECs of these dications, it can be easily deduced that a change

in the dynamics of these states would alter the KER features by about one electron volt or more, by the energy separation between asymptotic limits of the dications, which is not the case.

In Fig. 2, the asymptotic limits of the dications are shown as different lines on which the PECs are falling. KER values associated with PECs of the dications of  $N_2$  and  $CO$  are plotted with respect to the transition energy  $\epsilon$ . KER and transition energy,  $\epsilon$ , for a given PEC are related by a linear equation:

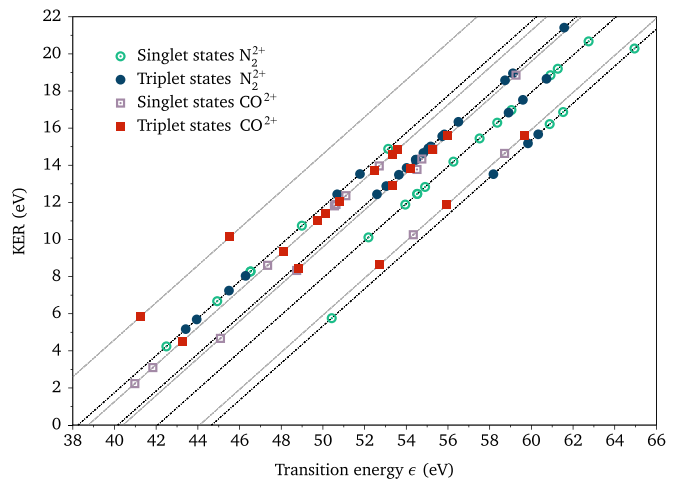


FIG. 2. KER values associated with PECs of the dications of  $N_2$  and  $CO$  are plotted with respect to the transition energy  $\epsilon$ . KER and transition energy for a given PEC are related by a linear equation:  $KER = \epsilon - a$ , where  $a$  is energy of the associated asymptotic limit. Each dot in the plot represents one PEC; the  $\epsilon$  is the vertical transition energy: energy difference between ground state of the molecule from the excited PEC of the dication. KER value represents the resulting dissociation energy via direct decay from the PEC. Consequently, PECs of a dication leading to a common asymptotic limit,  $a$ , appear on a straight line. Asymptotic limits of  $N_2^+$  are shown by dotted-dashed lines and of  $CO_2^+$  are shown by dashed lines.

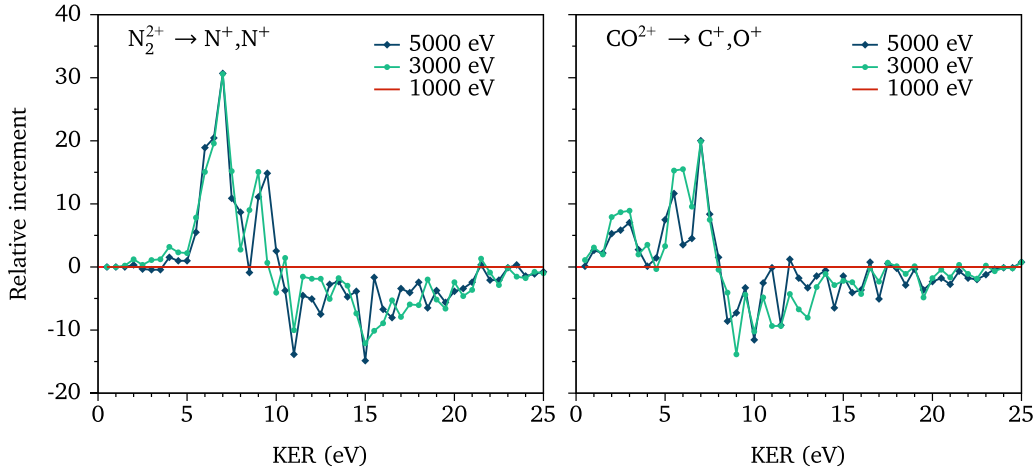


FIG. 3. Cross sections of the KER spectra of dissociation channel  $N_2^{2+} \rightarrow N^+, N^+$  [left] and  $CO^{2+} \rightarrow C^+, O^+$  [right] at electron-impact energies 3 and 5 keV compared with KER spectra at 1 keV are shown. If transition probability is a uniparameter function of transition energy, the difference spectra would be constant. The observed common trend in dissociation kinematics suggests that transition probability is also a function of the impact energy.

$KER = \epsilon - a$ , where  $a$  is the energy of the associated asymptotic limit. KERs, transition energies, and asymptotic limits are estimated using previous calculations of the PECs of these dications, reported in Pandey *et al.* [12]. These calculations were performed using MOLPRO program package [34]. Using correlation-consistent cc-pV5Z basis sets of N, C, and O, complete active space self-consistent field (CASSCF) method and multireference configuration interaction (MRCI) method have been used for calculations. Full-valence type CASSCF wave functions have been employed as the reference function in the MRCI calculations. The details of the calculation can be found in Pandey *et al.* [12]. KER originating from indirect pathways are not shown in Fig. 2. Indirect dissociation channels would appear as additional points in the same range bounded by the lowest and highest asymptotic limits. Since the dissociation dynamics is unaltered at different impact energies, these additional points would be identical in all cases and will not cause the observed trend in the difference KER spectra shown in Fig. 3.

In Fig. 3, cross sections of KER spectra of dissociation channel  $N_2^{2+} \rightarrow N^+, N^+$  and  $CO^{2+} \rightarrow C^+, O^+$  observed at electron-impact energies 3 and 5 keV are compared with KER spectra observed at 1 keV. Since these are differences drawn from normalized KER spectra, it can be easily seen that the relative cross section in low-KER range increases and as a result less cross section is seen in high-KER range. In the case of  $N_2^{2+}$ , below 10 eV, relative cross sections in 3, 5 keV impact cases become positive with respect to the KER spectra at 1 keV, whereas in case of  $CO^{2+}$ , 8 eV is the KER value below which relative cross sections become positive. To compare the variation in the relative cross sections, these KER values can be used as a marker. In the case of  $N_2^{2+}$ , for 3 and 5 keV electron-impact case, the average increase of cross section below 10 eV is about 8%. For  $CO^{2+}$ , the average cross section below 8 eV increases by about 6%.

As discussed in the experimental section, the first two cases of artifacts would not be the reason for the relative change of the cross sections when comparing for different electron-impact energies. The third experimental condition,

the statistical error of the recorded spectra, could contribute to some extent in this result. However, as discussed previously, the statistical error for the relevant range of the KER spectra in both cases is less than 10%, which is small compared to the observed change in the cross section. It is also interesting that the magnitude of changes in KER cross sections for 3 and 5 keV with respect to 1 keV are large compared to the relative change between 3 and 5 keV.

The transition probability,  $d\sigma$ , as a function of transition energy,  $\epsilon$ , and electron-impact energy,  $E$ , is given in Eq. (1). The transition probability in Eq. (1) is derived for fast moving electron collisions in atomic systems [6]:

$$d\sigma = \pi Z e^4 \left[ \frac{1}{\epsilon^2} + \frac{1}{(E - \epsilon)^2} - \frac{1}{\epsilon(E - \epsilon)} \right] \frac{d\epsilon}{E}. \quad (1)$$

The second term in Eq. (1) can be dropped for the impact energies which we have selected in our experiments. For the range of energy covering the transition energies of dications, relative increment in the normalized transition probabilities at 3 and 5 keV impact energies are compared with respect to the 1 keV case and is shown in Fig. 4. Transition probabilities for each impact energy are normalized to the 40–60 eV transition energy range in order to establish a comparison with the difference KER spectra shown in Fig. 3. It can be observed that the relative cross section for 3 and 5 keV with respect to the 1 keV impact case is smaller in low transition energy range, up to 48.75 eV; above this value the relative transition probability is larger. This suggests that the higher range in the KER spectra would be slightly more populated for larger impact energies. The predicted nature of the relative cross section is opposite to the nature which has been observed from the KER analysis. It is also evident that only a minor change would occur in the transition probability for three impact energies in the doubly ionized transition energy range. The maximum change in the transition probabilities are occurring at 40 eV and 60 eV transition energies; these are about 8 and 12 units, respectively, in the same scale in which the difference KER spectra in Fig. 3 are plotted.

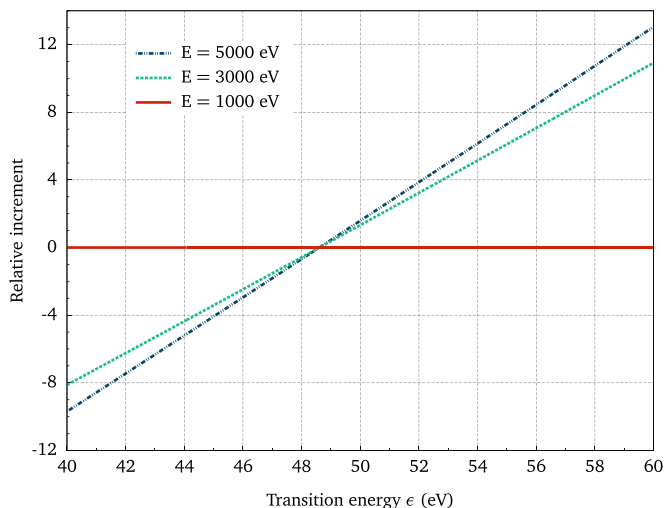


FIG. 4. Relative increment in the normalized transition probabilities at 3 and 5 keV impact energies are compared with respect to the 1 keV case. Transition probabilities for each impact energy are normalized to the 40–60 eV transition energy range in order to establish a comparison with the difference KER spectra shown in Fig. 3. It can be observed that the relative cross section for 3 and 5 keV with respect to 1 keV impact case is smaller in the low transition energy range, up to 48.75 eV; above this value the relative transition probability is larger.

Our observation suggests that the transition probability would be a weak function of the impact energy  $E$ , but the dependence is stronger than it is predicted by Eq. (1) [6]. It is hard, though, to discern the exact form of the function, but the observed trend suggests that it would be a decreasing function that may appear as an additional term, possibly in  $(E-\epsilon)$  form, in the transition probability equation. The observed trend is

opposite to the predicated nature of the relative increments in cross section for different impact energies. Equation (1) is using two assumptions that might be the reason for the observed deviation. It considers the transition energy as the energy gained by the ionizing electron in collision and does not take into account the effects of collision on remaining  $Z - 1$  electrons in the system; multiple excitation in the collision may be a contributing factor. Equation (1) also considers a single-centered Coulomb field and is derived for atomic systems; a two-centered Coulomb field is another possible factor for the observed change. Our work provides further insights about the dissociation dynamics of the molecules; in this article, the nature of the excitation in a dissociative ionization process is addressed.

#### IV. CONCLUSIONS

In this paper, we have analyzed KER spectra of CSD channels of dications of  $N_2$  and CO molecules for three electron-impact energies, viz. 1, 3, and 5 keV. KER spectra, which is a measure of the undergoing dissociation dynamics, observed at different impact energies are compared. To make a comparative study, experiments were performed in identical conditions and all the experimental parameters have been considered and their effects have been evaluated to ensure that the observed differences in the KER spectra are significant and are not due to experimental artifacts. The observed result suggests that the transition probability should be a decreasing function of the impact energy of the projectile. Multiple electronic excitation and many-centered Coulomb field are the possible contributing factors in the transition probability. More experimental observations at many impact energies especially in the low-energy range, between 1000 and 200 eV, as well as for many other molecular systems may reveal the specificity of the transition probability as a function of the impact energy.

- 
- [1] M. Born and R. Oppenheimer, *Ann. Phys. (NY)* **389**, 457 (1927).
- [2] A. Szabo and N. S. Ostlund, *Modern Quantum Chemistry: Introduction to Advanced Electronic Structure Theory* (Courier Dover Publications, New York, 2012).
- [3] I. N. Levine, *Quantum Chemistry* (Prentice-Hall Upper Saddle River, NJ, 2000), Vol. 5.
- [4] D. Mathur, *Phys. Rep.* **391**, 1 (2004).
- [5] J. Ullrich and V. Shevelko, *Many-particle Quantum Dynamics in Atomic and Molecular Fragmentation* (Springer, New York, 2003).
- [6] L. D. Landau and E. M. Lifshitz, *Quantum Mechanics Non-relativistic Theory* (Pergamon Press, New York, 1991), Vol. 3.
- [7] H. C. Straub, P. Renault, B. G. Lindsay, K. A. Smith, and R. F. Stebbings, *Phys. Rev. A* **52**, 1115 (1995).
- [8] D. J. Haxton, *Phys. Rev. A* **88**, 013415 (2013).
- [9] D. Rapp, P. EnglanderGolden, and D. D. Briglia, *J. Chem. Phys.* **42**, 4081 (1965).
- [10] Y. Itikawa, *J. Phys. Chem. Ref. Data* **35**, 31 (2006).
- [11] W. Hwang, Y. Kim, and M. E. Rudd, *J. Chem. Phys.* **104**, 2956 (1996).
- [12] A. Pandey, B. Bapat, and K. R. Shamasundar, *J. Chem. Phys.* **140**, 034319 (2014).
- [13] Z. Wu, C. Wu, X. Liu, Y. Deng, Q. Gong, D. Song, and H. Su, *J. Phys. Chem. A* **114**, 6751 (2010).
- [14] P. Lablanquie, J. Delwiche, M.-J. Hubin-Franskin, I. Nenner, P. Morin, K. Ito, J. H. D. Eland, J.-M. Robbe, G. Gandara, J. Fournier, and P. G. Fournier, *Phys. Rev. A* **40**, 5673 (1989).
- [15] M. Lundqvist, D. Edvardsson, P. Baltzer, and B. Wannberg, *J. Phys. B* **29**, 1489 (1996).
- [16] J. Rajput, S. De, A. Roy, and C. P. Safvan, *Phys. Rev. A* **74**, 032701 (2006).
- [17] K. Boyer, T. S. Luk, J. C. Solem, and C. K. Rhodes, *Phys. Rev. A* **39**, 1186 (1989).
- [18] C. Cornaggia, J. Lavancier, D. Normand, J. Morellec, and H. X. Liu, *Phys. Rev. A* **42**, 5464 (1990).
- [19] I. Ben-Itzhak, S. G. Ginther, and K. D. Carnes, *Phys. Rev. A* **47**, 2827 (1993).
- [20] C. Tian and C. R. Vidal, *Phys. Rev. A* **59**, 1955 (1999).
- [21] K. Wohrer, G. Sampoll, R. L. Watson, M. Chabot, O. Heber, and V. Horvat, *Phys. Rev. A* **46**, 3929 (1992).
- [22] T. Masuoka and E. Nakamura, *Phys. Rev. A* **48**, 4379 (1993).

- [23] T. Masuoka, *J. Chem. Phys.* **101**, 322 (1994).
- [24] T. Osipov, T. Weber, T. N. Rescigno, S. Y. Lee, A. E. Orel, M. Schöffler, F. P. Sturm, S. Schössler, U. Lenz, T. Havermeier *et al.*, *Phys. Rev. A* **81**, 011402 (2010).
- [25] M. Lundqvist, P. Baltzer, D. Edvardsson, L. Karlsson, and B. Wannberg, *Phys. Rev. Lett.* **75**, 1058 (1995).
- [26] M. Tarisien, L. Adoui, F. Frémont, D. Lelièvre, L. Guillaume, J.-Y. Chesnel, H. Zhang, A. Dubois, D. Mathur, S. Kumar *et al.*, *J. Phys. B* **33**, L11 (2000).
- [27] W. Wiley and I. McLaren, *Rev. Sci. Instrum.* **26**, 1150 (1955).
- [28] V. Sharma and B. Bapat, *Eur. Phys. J. D: At., Mol., Opt. Plasma Phys.* **37**, 223 (2006).
- [29] A. K. Pandey, Ph.D. thesis, Mohanlal Sukhadia University Udaipur, 2014, [http://www.iiserpune.ac.in/~bhasbapat/bapat\\_files/thesis-amrendra.pdf](http://www.iiserpune.ac.in/~bhasbapat/bapat_files/thesis-amrendra.pdf).
- [30] A. Pandey and B. Bapat, *Int. J. Mass Spectrom.* **361**, 23 (2014).
- [31] E. Liénard, M. Herbane, G. Ban, G. Darius, P. Delahaye, D. Durand, X. Fléchar, M. Labalme, F. Mauger, A. Mery *et al.*, *Nucl. Instrum. Methods Phys. Res., A* **551**, 375 (2005).
- [32] G. Fraser, *Int. J. Mass Spectrom.* **215**, 13 (2002).
- [33] I. Ali, R. Dörner, O. Jagutzki, S. Nüttgens, V. Mergel, L. Spielberger, K. Khayyat, T. Vogt, H. Bräuning, K. Ullmann *et al.*, *Nucl. Instrum. Methods Phys. Res., B* **149**, 490 (1999).
- [34] H.-J. Werner, P. J. Knowles, G. Knizia, F. R. Manby, and M. Schütz, *WIREs Comput. Mol. Sci.* **2**, 242 (2012).